Available online at www.sciencedirect.com
ScienceDirect
Acta Materialia 59 (2011) 3680–3687
Acta MATERIALIA
www.elsevier.com/locate/actamat

Interpreting hydrogen-induced fracture surfaces in terms of deformation processes: A new approach

M.L. Martin [a], I.M. Robertson [a,*], P. Sofronis [b]

[a] Department of Materials Science and Engineering, University of Illinois, Urbana-Champaign, IL, USA
[b] Department of Mechanical Science and Engineering, University of Illinois, Urbana-Champaign, IL, USA

Received 15 December 2010; received in revised form 27 February 2011; accepted 4 March 2011

Abstract

Interpreting topological features on fracture surfaces in terms of the underlying deformation processes has traditionally been based on assumed knowledge of the processes and mechanisms with no direct correlation being established. By using a combination of high-resolution scanning electron microscopy (SEM), atomic force microscopy and focused-ion beam machining to enable investigation by transmission electron microscopy of the microstructure immediately beneath the surface, correlation of developed structure with the topology of the fracture surface becomes possible. Using this methodology, features on hydrogen-induced fracture surfaces that appear flat at low resolution under SEM are revealed to be decorated with fine-scale undulations that are associated with an underlying dense arrangement of dislocations. The formation of this microstructure and the fracture surface are discussed in terms of hydrogen embrittlement models, with the conclusion reached that the surface formation can be understood within the framework of the enhanced plasticity model of hydrogen embrittlement establishing the conditions that favor the formation of the observed surface features.

Keywords: Hydrogen embrittlement; Fracture; Scanning electron microscopy; Transmission electron microscopy

1. Introduction

The phenomenon of hydrogen embrittlement of iron and steel has been known since 1874 [1]; it appears as a loss of toughness that can result in a sudden catastrophic failure of components at loads significantly below the design load. The loss of ductility is frequently accompanied by a change in fracture mode from ductile rupture to cleavage or to intergranular failure. In non-hydride-forming systems, these changes are described commonly in terms of one of the following models:

- The decohesion model, which is based on hydrogen causing a reduction in the strength of atomic bonds [2–9].
- The hydrogen-enhanced dislocation emission model in which hydrogen lowers the surface energy, and this facilitates the injection of dislocations from the surface [10,11].
- The hydrogen-enhanced localized plasticity mechanism in which the hydrogen atmosphere attached to the dislocation effectively lowers the interactions with elastic obstacles, which means that the shear stress for dislocation motion is reduced [12–24].

However, with the exception of the hydrogen-enhanced plasticity model, there is a paucity of direct experimental evidence for the other mechanisms [12]. The "experimental evidence" supporting them is associated with a posteriori interpretation of macroscopic tests and observations. That is, the underlying physical processes responsible for the macroscopic effect are interpreted based on anticipated and expected deformation responses rather than through direct observation. Alternatively, they are based on simula-

* Corresponding author.
E-mail address: ianr@illinois.edu (I.M. Robertson).

1359-6454/$36.00 © 2011 Acta Materialia Inc. Published by Elsevier Ltd. All rights reserved.
doi:10.1016/j.actamat.2011.03.002

tions and models that consider simple and ideal situations that remain to be validated experimentally.

The decohesion mechanism, for example, was founded initially on the interpretation of features on the fracture surface [2,4,5]. In this interpretation, it was assumed that any plasticity that occurred was a direct consequence of the actual embrittlement mechanism rather than being an integral component of it. That is, it was a result, not the cause, of the embrittlement. Later, this position was changed to include plastic processes as a component in the embrittlement process [9,25–29]. For example, in their explanation of hydrogen-induced cleavage in Fe–Si single crystals, Gerberich and coworkers included slip on well-defined slip planes emanating from the crack tip to generate the high stresses such that the location of the theoretical fracture stress moved to within a few tens of nanometers of the crack tip [9,25]. With the generation of this high stress there would be an accompanying enhancement of the hydrogen concentration such that it could cause a significant reduction in the lattice cohesive strength. Vehoff and Neumann presented evidence for the occurrence of ductile processes in a Fe–2.6% Si single crystal although they reached the conclusion that "plasticity may be responsible in a yet unknown way for the stable quasi-brittle crack growth" [26]. More recently, Vehoff and coworkers have attributed enhanced dislocation production by hydrogen to how it changes the shear modulus, dislocation core and stacking-fault energy [28]. Although direct measurement of the change in cohesive strength as a function of hydrogen concentration is not available, there is indirect experimental evidence in support of such an effect. For example, the increased fraction of intergranular failure that occurs in some systems as the hydrogen concentration at the grain boundary increases [30–37], the initiation of voids and microcracks at the interface between precipitates and the matrix, and the sudden loss of ductility at high hydrogen concentrations in a β-Ti alloy [38], support a reduction in the cohesive strength. Ab initio calculations support hydrogen reducing the cohesive strength of the lattice, although there remains uncertainty as to the specific relationship, linear or nonlinear, between hydrogen concentration and the magnitude of the reduction in the cohesive strength [39–42]. Here predictions of some models must be treated with caution as the calculations are for equilibrium conditions [43,44], which is not the case for transgranular fracture events, and other processes may have activated before the conditions under which hydrogen-induced decohesive failure occurs. Other mechanisms, such as the hydrogen-enhanced emission of dislocations from surfaces, which was based on the similarities of fracture surfaces in liquid metal and hydrogen embrittled metals, lack direct evidence for enhanced surface emission due to hydrogen [11,45].

In this paper, the underlying microstructure of a common feature on hydrogen-induced fracture surfaces of a steel, namely flat "featureless" regions, is discovered by using a combination of techniques that span multiple length scales. These surfaces were interpreted as evidence for hydrogen-enhanced decohesion, but, through the use of high-resolution scanning electron microscopy (SEM) and atomic force microscopy (AFM), as well as transmission electron microscopy (TEM) examination of the volume immediately beneath the fracture surface, it will be demonstrated that neither the topology of the fracture surface nor the underlying microstructure are consistent with a classical decohesion mechanism.

2. Experimental procedure

The materials used in this study were API grade X80 and X60 HIC pipeline steels. These steels have a yield strength of 565 and 434 MPa, respectively. Somerday and coworkers conducted compact tension tests on these materials under high hydrogen gas pressures and found that hydrogen caused a reduction in the toughness of both steels [46,47].

The fracture surfaces of samples obtained from Dr. B. Somerday were examined by SEM: low-resolution analysis was conducted by using a JEOL JSM-6060LV SEM or by using the electron mode of a FEI 235 focused-ion beam (FIB) microscope. High-resolution images were taken using a JEOL 7000F SEM. The surface morphology was examined by AFM using a Digital Instruments Dimension 3100 microscope operated in tapping mode.

TEM samples were machined from site-specific locations of the fracture surface using the FIB lift-out technique. Previous TEM studies have shown that the fracture surface is preserved in this process and the resulting thinning to electron transparency by ion milling yields a sample that is uniformly thick, with a thickness of between 100 and 300 nm [48,49]. The sample thickness and its uniformity over the viewing area, from the fracture surface to micrometers into the material, negate most of the concerns regarding rearrangement and loss of dislocation structures in the thinnest regions of electron-transparent samples. These samples were examined in a JEOL 2010LaB_6 TEM operated at 200 kV or at Argonne National Laboratory using a Hitachi H9000 TEM operated at 300 kV.

3. Results

Examples of the different morphologies found on the hydrogen-induced fracture surface are shown in the fractographs presented in Fig. 1. Several features can be identified, including secondary cracks, cracks at inclusions, "quasi-cleavage" and flat "featureless" regions. These latter surfaces and the microstructure beneath them are the focus of this effort; the "quasi-cleavage" surface has been described in detail elsewhere [48].

The flat fracture surfaces are examined in detail in the fractographs presented in Figs. 2 and 3. The dimensions of these regions are equivalent to the grain size (5 μm), although larger (up to 20 μm) flat areas exist. On closer

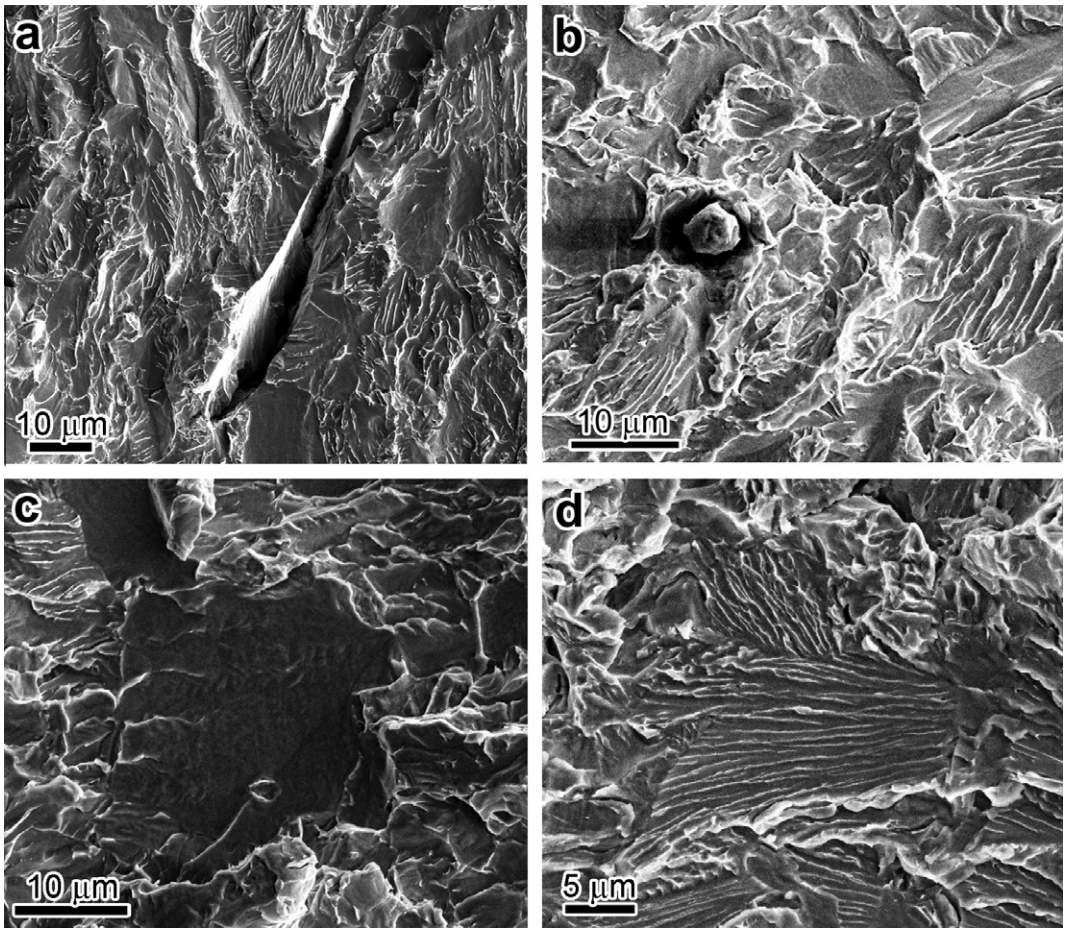

Fig. 1. SEM images showing typical features of fracture surface: (a) secondary cracking; (b) inclusion; (c) flat features; (d) quasi-cleavage features.

inspection, it can be seen that these larger flat regions are composed of multiple grains that fail in a coplanar manner. The flat features are either rounded or irregular in shape, with upward sloping sides often leading to shear lips at the periphery. SEM examination of these surfaces reveals that they are not flat but on a large scale are undulating (Fig. 2b). These undulations are more evident in the topological image of the fracture surface, reconstructed using the software MeX by Alicona, presented in Fig. 2c. Therefore, the first point to note is that these surfaces are not flat.

Higher-resolution fractographs show that superimposed on the undulations are what appear to be small (~50 nm diameter) rounded mounds (Fig. 3b); the lower-resolution image of the same areas is shown for comparison in Fig. 3a and it is clear these features are not resolved at such resolution. The roughness of this surface is confirmed by the AFM images and measurements. An example of an AFM image is presented in Fig. 4a; it shows the overall roughness of the surface, which is consistent with the SEM images presented in Fig. 3. The height measurements taken in different directions on the surface show height differences of 5 nm between mounds that are 50 nm in diameter. The second point to note is that the surface is covered with a high density of these small mounds.

To determine the origin of this surface topology, samples for examination in a TEM were extracted normal to the surface and thinned such that the volume immediately beneath it could be examined. Examples of the microstructure found immediately beneath the fracture surface are shown in Fig. 5. In each micrograph, the position of the platinum strip deposited to protect the surface during the extraction process is indicated. The fact that this strip remains intact confirms that the fracture surface is indeed preserved for examination; that this is the case was confirmed in other studies in which the surface features were preserved and is evident from the electron microscopy investigations [48,49]. As is evident from these bright-field micrographs, a high density of dislocation lines and loops exists immediately beneath the surface. The overall dislocation density and distribution with distance from the fracture surface is shown in the micrographs presented in Fig. 5a and b, and specific features, such as the dislocation loops within a select region, are shown in the insets. The dislocation structure is not confined to near the fracture surface, but extends over 1500 nm from it (Fig. 5b). Furthermore, there is no discernible gradient in the density of dislocations with distance from the fracture surface. That this is the case can be seen by comparing the micro-

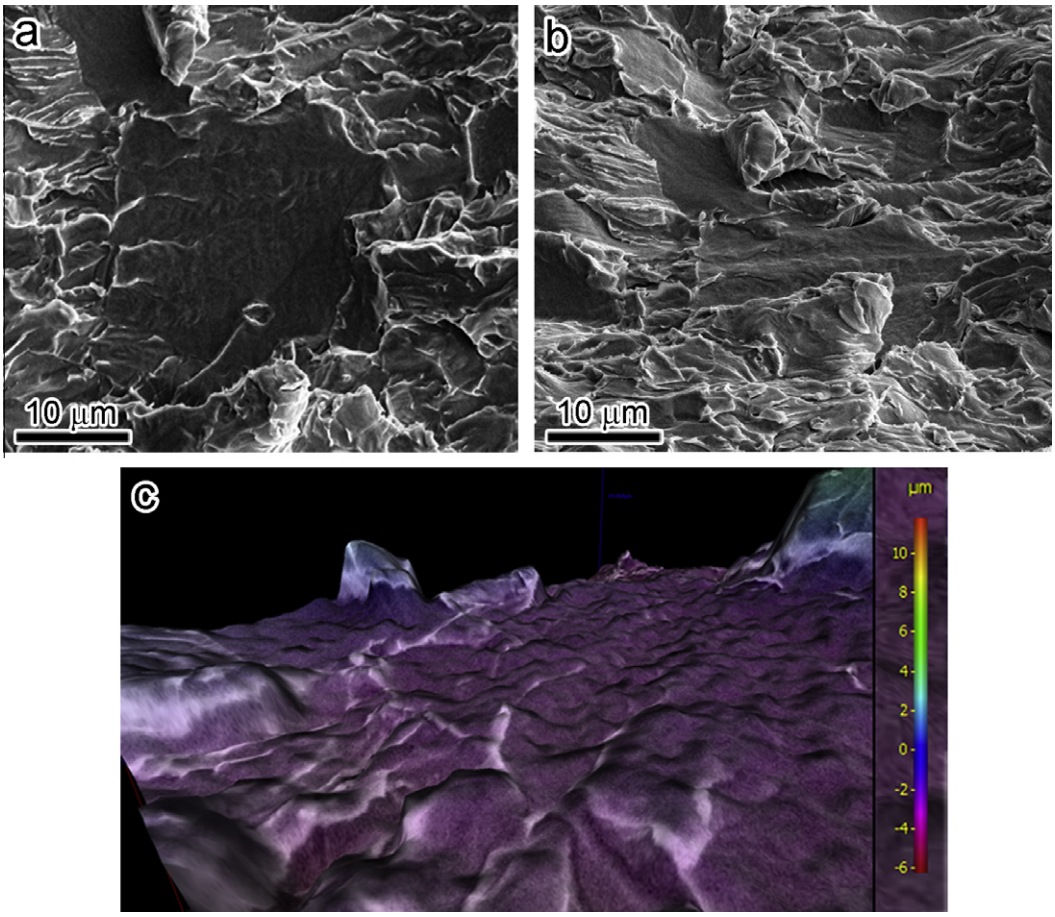

Fig. 2. SEM images showing the flat fracture surface at (a) 0° tilt and (b) 52° tilt; (c) three-dimensional reconstructed image of the same feature showing the surface roughness.

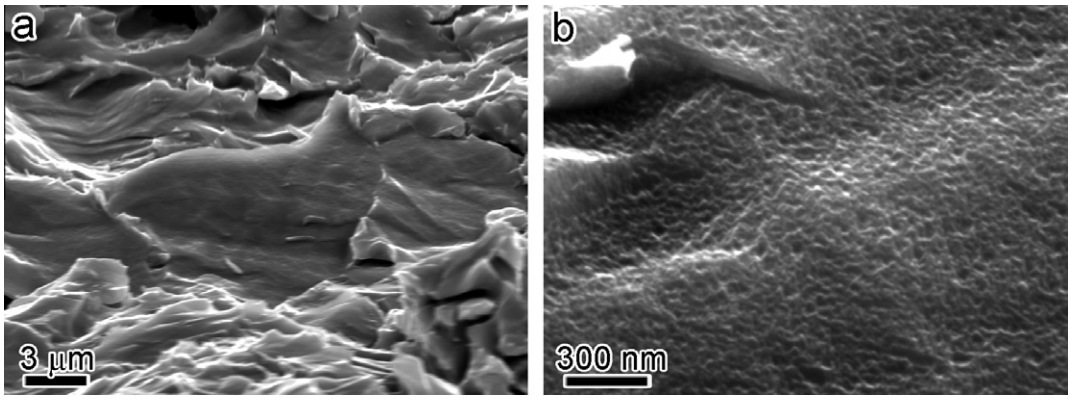

Fig. 3. (a) SEM image showing flat feature; (b) high-magnification image showing the mounds covering the surface.

graph in Fig. 6, which is of the near-surface region, with the higher magnification images of the boxed regions presented in Fig. 5a and b, which represent the structure at depths of 250 and 1500 nm from the fracture surface, respectively. In some micrographs, the viewed area is divided by a grain boundary; the dislocation density does not appear to be affected by the presence of these boundaries but extends unperturbed into the next grain. While precipitates, such as the cementite particles shown in Fig. 7, were observed in the vicinity of the fracture surface, they did not appear to influence the topology.

Electron backscatter diffraction was employed in an attempt to determine the plane of the fracture. Unfortunately, the undulations, mounds and extensive plasticity immediately beneath the surface precluded obtaining patterns that could be analyzed with confidence. Furthermore, although electron diffraction patterns were obtained during the electron microscopy analysis, it was not possible to

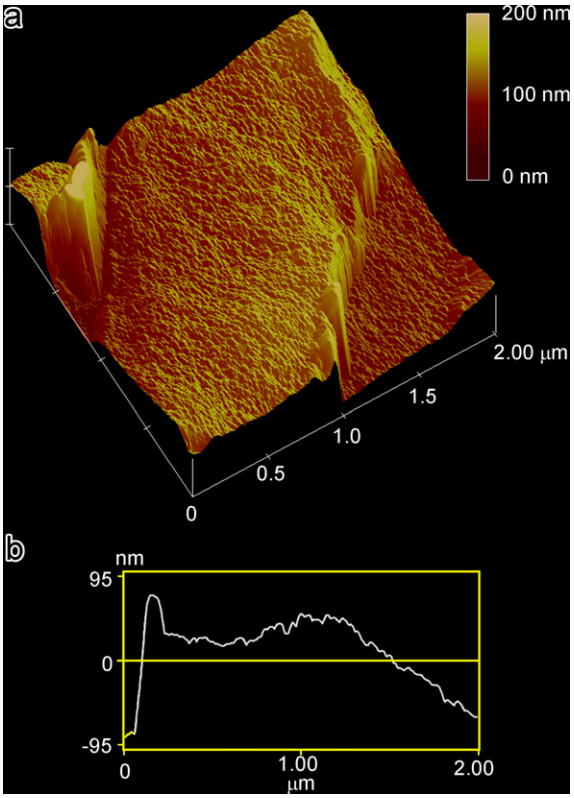

Fig. 4. (a) Depth map generated from AFM of flat fracture region. (b) Line scan horizontally across showing roughness. Line scans in other directions were comparable.

determine unambiguously the normal of the fracture plane from them because of the roughness and the attendant error associated with not having the fracture plane normal to the beam direction over an appropriate angular range. Therefore, the fracture plane could not be determined.

4. Discussion

It has been shown for the first time that the fracture surface, which appears at low resolution to be relatively flat, is actually undulating and covered with small mounds. The microstructure immediately beneath this surface consists of a high density of dislocation lines and loops, the density of which remains constant and unchanged through multiple grains that extend to distances of many micrometers. This observation, along with the identification of slip bands as playing a prominent role in the formation of "river markings" decorating hydrogen-induced "quasi-cleavage" fracture surfaces, raises questions about interpreting the relationship between the deformation processes and failure mechanisms and the macroscopic topology of fracture surfaces without knowledge of the actual microstructure.

In the case of the formation of "quasi-cleavage" surfaces, Martin et al. demonstrated that the ridges forming the river markings were aligned with slip bands [48]. They rationalized that the surface was generated by the growth and extension of voids that nucleated at and along intersections of intense slip bands. Void growth occurred via plastic processes. The role of hydrogen was to assist in the formation of the intense slip bands, to promote void formation at and along the intersection because of higher concentrations, and to accelerate the growth by dislocation processes. From the correlation of the topology of the fracture surface with the underlying microstructure, Martin et al. concluded that the formation of "quasi-cleavage" fracture surfaces was not associated closely with cleavage-like processes, as the name might imply, but to plastic deformation processes that are enhanced by hydrogen [48]. The difference in the dislocation structure beneath the "quasi-cleavage" and the surface described herein reflects the difference in grain orientation and its effect on the relationship between the local stress state and the deformation mode.

Lynch has suggested that similarities in the appearance of fracture surfaces in liquid metal and hydrogen embrittlement point to a common mechanism in which changes in the surface energy promote the formation and injection of dislocations from the surface into the material [10,11]. If this was the operative mechanism, a gradient in the dislocation density from the fracture surface would be anticipated and half-loop structures should emanate from it. However, as is evident from the electron micrographs presented in Figs. 5 and 6, dislocation half-loops are not seen emerging from the fracture surface, there is no obvious gradient in the dislocation density with distance from the surface, and a uniform dislocation density extends through multiple grains from the fracture surface. These results suggest that in this case there is no enhanced dislocation emission from surfaces. Of course, it always could be argued that the dislocation structure generated initially prohibits identification of the dislocations produced by the advancing crack, but, as there is no modification to the structure, especially near the surface, this seems improbable. Furthermore, recent studies probing the microstructure immediately beneath a liquid metal embrittled steel indicates different processes may be active despite some similarities, at least, at low resolution, of the fracture surfaces generated by the two environments [50]. That is, the surfaces resulting from the different embrittling agents appear similar at low resolution, but the underlying processes responsible for inducing the failure are different.

Another mechanism that is often invoked to explain hydrogen embrittlement is decohesion, essentially a reduction in the bond strength due to the presence of hydrogen [2–9]. In the earliest explanations of decohesion models, it was suggested that any plastic processes were an after-effect of the critical hydrogen embrittlement event. For example, in stress-relaxation studies conducted in 1045 steel, the hydrogen-induced growth of voids by decohesion caused a change in the internal stresses that caused plasticity and the observed stress relaxation [4]. On fracture surfaces, any evidence of plasticity was explained to be a consequence of the embrittlement event. If the fracture surface observed in this work was simply a consequence of a

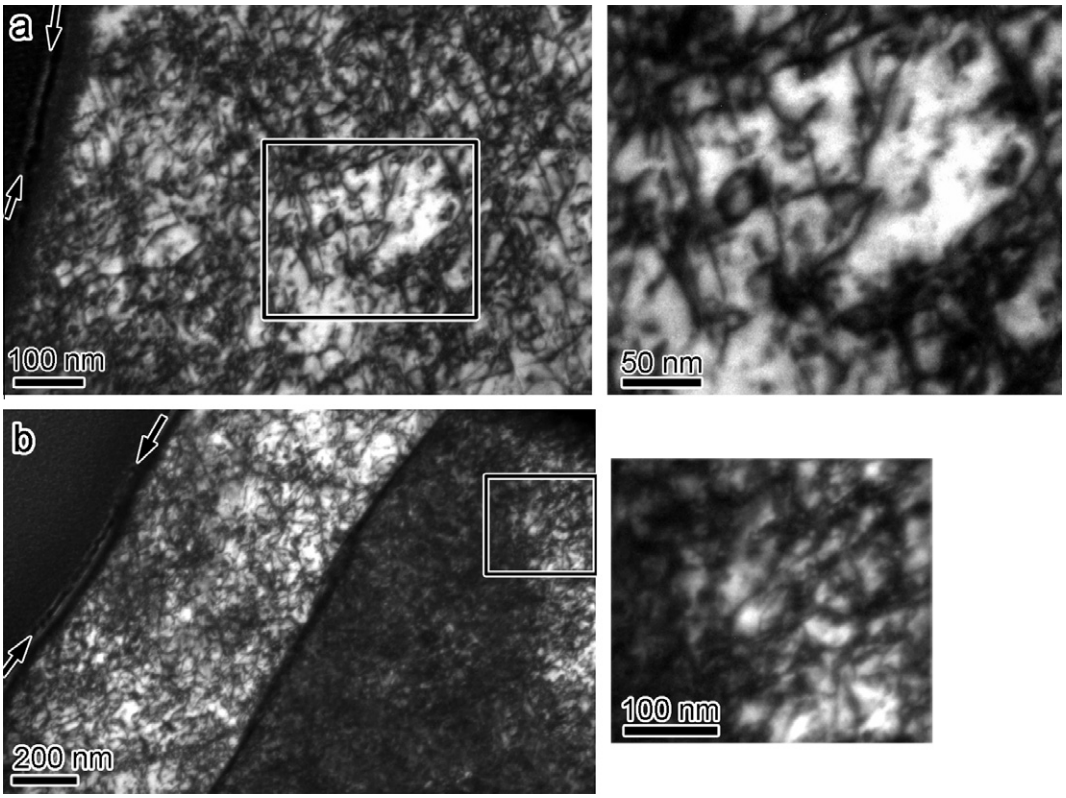

Fig. 5. TEM micrographs showing the microstructure present directly below the fracture surface. (a and b) Dislocation density immediately below the surface of two different flat features. Selected areas magnified on right. The micrographs shown in the insets are from regions at depths of 250 and 1500 nm from the fracture surface, respectively.

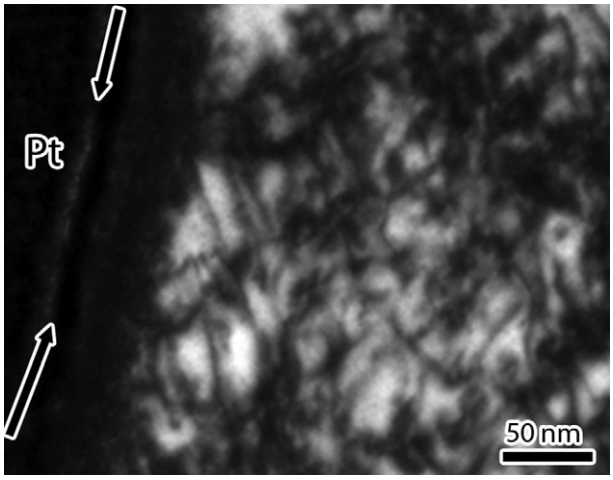

Fig. 6. Bright-field micrograph showing dislocation density in the near-surface region of the fracture surface.

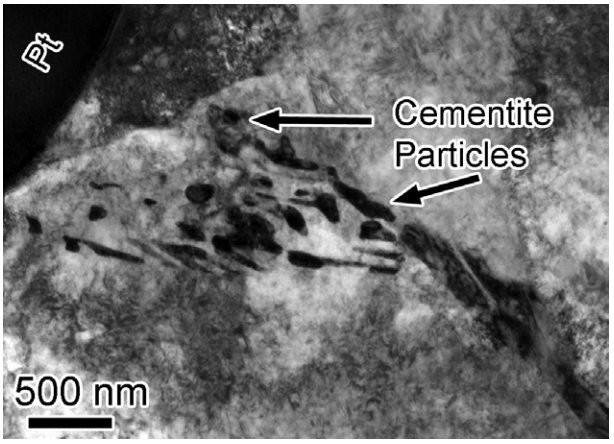

Fig. 7. Bright-field micrograph showing cementite particles immediately below fracture surface, but not influencing fracture morphology.

decohesion event accompanied by a release of dislocations, a gradient in the dislocation density would be anticipated. That is, the dislocation density would be highest near the surface and decrease with distance from it. The present TEM results show no evidence consistent with dislocation emission from the surface or of a gradient in dislocation density, which suggests that in this case the decohesion mechanism accompanied by an injection of dislocations is not active.

Later explanations of decohesion included plasticity processes. In general, these were used to transport hydrogen from the crack surface to the interior of the specimen where it was deposited at the interior traps such as precipitates or grain boundaries—this is essentially the Hirth model of embrittlement that has been invoked to explain

the formation of some fracture surfaces [32]. Others have introduced plasticity as a means to accentuate the local stress field around the crack tip such that the associated stress enhancement of hydrogen is locally significant [9,25,51]. These hydrogen-associated plasticity processes, as will be described below, are different from those envisioned to be active in the formation of the fracture surface features shown in Figs. 2 and 3.

The hydrogen-enhanced localized plasticity mechanism purports that hydrogen segregates to and accumulates in the stress fields of dislocations and other elastic defects where it causes a modification in the dislocation–defect interactions such that they are diminished in some directions and accentuated in others (e.g. in the case of a moving dislocation when it meets a carbon atom impurity). One case in which this interaction is reduced is between two edge dislocations along the slip plane. This means that the dislocation interactions and reactions are similar in the presence and in the absence of hydrogen, but occur at lower stresses when hydrogen is present. Since hydrogen is attached to and transported with the dislocations, locally high hydrogen concentrations should exist in regions of high dislocation density. To link the underlying microstructure to the crack path and the topology of the fracture surface, it is posited that the dislocation structure, which is established well in advance of the crack with the aid of the hydrogen-enhanced plasticity mechanism and the local hydrogen concentration associated with the dislocations, establishes local conditions that promote fracture. The undulations and mounds are most likely a consequence of either near-surface relaxations associated with the formation of new surfaces or reflect the underlying dislocation structure and local high hydrogen concentration. That is, the far-field dislocation structure and the attendant hydrogen concentration establish weak regions, which dictate the local crack path and the topology of the resulting fracture surface. Consequently, it is unlikely that there is a unique fracture plane as it is determined by the interplay between local conditions and the stress conditions.

The posited mechanism has implications for the application of continuum plasticity models to hydrogen embrittlement. Assuming the yield strength of the steel is 500 MPa and the stress intensity factor at failure is 90 MPa $m^{1/2}$, then from continuum plasticity the crack opening displacement is calculated as 44×10^{-6} m in the absence of hydrogen. Taking the fracture process zone as three times the crack opening displacement yields a process zone size of 120×10^{-6} m with the maximum stress located approximately at 88×10^{-6} m. At this location, the lattice hydrogen concentration is enhanced approximately by a factor of 3 over the bulk lattice concentration, C_o. Furthermore, the dislocation stress fields may enhance the hydrogen concentration by a factor of 10–90C_o. The SEM images presented in Figs. 2 and 3 yield a grain size of about 5×10^{-6} m; therefore, at least four grains in the volume ahead of the crack tip are strained intensely. These calculations neglect any influence of hydrogen on the deformation processes and the local hydrogen concentration as affected by the dislocation motion. As noted earlier, hydrogen is transported by mobile dislocations and within the framework of the hydrogen-enhanced localized plasticity mechanism will lead to the plasticity being extended to additional grains in at least some directions. That is, the dislocation microstructure should extend through multiple grains in the three-dimensional volume ahead of the crack tip. This is consistent with the evidence presented in Fig. 5 in which high dislocation densities are seen extending without any obvious gradient from the fracture surface over multiple grains. It also does not contradict the fact that continuum plasticity predicts, in the absence of hydrogen, severe straining over eight grains from the crack tip. Two important effects need to be taken into account: the influence of hydrogen on the dislocation mobility and the impact of hydrogen transport by mobile dislocations on the hydrogen distribution. Within the framework of the posited mechanism, for the same level of stress, the dislocation density and hydrogen concentration will be higher in the plastic zone and the size of the plastic zone may be greater when hydrogen is present. In regions in which dislocation tangles form, the accompanying hydrogen atmospheres will superimpose to create locally high total hydrogen concentrations [23]. These concentrations may be sufficient to cause a significant reduction in the lattice cohesive strength, which would enhance the propensity for cracking in that locale even in advance of the primary crack. In other words, the evolved microstructure and hydrogen concentrations establish the conditions that dictate the macroscopic response. This is a very different scenario to that considered in classical continuum approaches or discretized dislocation approaches to model hydrogen embrittlement in which it is assumed the crack or the dislocations emitted from it are advancing into pristine material.

5. Conclusions

The microstructure immediately beneath a hydrogen-induced fracture surface has been revealed by using FIB machining to extract and produce an electron-transparent sample from a specific location. The microstructure, along with high-resolution fractographs and AFM images of the fracture surface, suggests that the underlying dislocation structure has a key role to play in establishing the conditions that ultimately determine the topology of the fracture surface. In this case, the role of hydrogen is to establish the dislocation substructure and the local hydrogen concentration, which increases the propensity for cracking in that specific location. The fine features on the fracture surface are most probably a consequence of relaxation events that occur because of the creation of new surfaces or simply reflect the path with the highest local hydrogen concentration.

It is proposed that the methodology adopted herein rather than the traditional a posteriori approach should be used to establish the link between microstructure and

fracture mode. Finally, it is proposed that these results, along with those reported by Martin et al. for the formation of quasi-cleavage fracture surfaces, suggest that continuum plasticity models for hydrogen/deformation interactions need to be revisited.

Acknowledgements

This work was supported by DOE grant GO15045. Microscopy work was carried out in part in the Center for Microanalysis of Materials in the Frederick Seitz Materials Research Laboratory at the University of Illinois. The authors would like to acknowledge the use of the IVEM-accelerator facility at Argonne National Laboratory and Dr. M.A. Kirk for assistance, support and discussion. This document was prepared by the University of Illinois at Urbana-Champaign as a result of the use of facilities of the US Department of Energy (DOE), which are managed by UChicago Argonne, LLC, acting under Contract No. DE-AC02-06CH11357. Neither UChicago Argonne, DOE, the US Government, nor any person acting on their behalf: (a) make any warranty or representation, express or implied, with respect to the information contained in this document; or (b) assume any liabilities with respect to the use of, or damages resulting from the use of any information contained in the document. The authors acknowledge and thank Dr. B. Somerday for the provision of the fracture samples and for fruitful discussions. I.M.R. acknowledges discussion with Professor C. Altstetter.

References

[1] Johnson WH. Proc Roy Soc Lond 1875;23:168.
[2] Oriani RA, editor. Hydrogen embrittlement of steels. Palo Alto, CA, USA: Annual Reviews Inc.
[3] Oriani RA. Corrosion 1987;43:390.
[4] Oriani RA, Josephic PH. Acta Metall 1979;27:997.
[5] [5] Oriani RA, Josephic PH. Scripta Metall 1979;13:469.
[6] Troiano AR. Trans Am Soc Met 1960;52:54.
[7] Troiano AR, Fidelle JP. Hydrogen embrittlement in stress corrosion cracking. In: International congress on hydrogen in metals. Paris; 1972.
[8] Gangloff RP. Science-based prognosis to manage structural alloy performance in hydrogen. In: Somerday B, Sofronis P, Jones R, editors. Effects of hydrogen on metals. Jackson Hole, WY: ASM International; 2009. p. 1. .
[9] Gerberich WW, Oriani RA, Lii MJ, Chen X, Foecke T. Philos Mag A, Phys Condens Matter Defects Mech Prop 1991;63:363.
[10] Lynch SP. Met Forum 1979;2:189.
[11] Lynch SP. Acta Metall 1988;36:2639.
[12] Robertson IM, Birnbaum HK, Sofronis P, editors. Hydrogen effects on plasticity. New York: Elsevier; 2009.
[13] Robertson IM, Lillig D, Ferreira PJ. Revealing the fundamental processes controlling hydrogen embrittlement. In: Somerday B, Sofronis P, Jones R, editors. Hydrogen in metals. Jackson Hole, WY: ASM International; 2009.
[14] Ahn DC, Sofronis P, Dodds R. Int J Fract 2007;145:135.
[15] Birnbaum HK, Sofronis P. Mater Sci Eng A, Struct Mater, Prop Microstruct Process 1993;A176:191.
[16] De Los Rios ER, Sun ZY, Miller KJ. Fatigue Fract, Eng Mater Struct 1994;17:1459.
[17] Delafosse D, Magnin T. Eng Fract Mech 2001;68:693.
[18] Tien CW, Altstetter CJ. Mater Chem Phys 1993;35:58.
[19] Beachem CD. Metall Trans 1973;4:1999.
[20] Chateau JP, Delafosse D, Magnin T. Acta Mater 2002;50:1507.
[21] Gavriljuk VG, Shivanyuk VN, Foct J. Acta Mater 2003;51:1293.
[22] Hanninen HE, Lee TC, Robertson IM, Birnbaum HK. J Mater Eng Perform 1993;2:807.
[23] Sofronis P, Birnbaum HK. J Mech Phys Sols 1995;43:49.
[24] Nibur KA, Bahr DF, Somerday BP. Acta Mater 2006;54:2677.
[25] Lii MJ, Chen XF, Katz Y, Gerberich WW. Acta Metall Mater 1990;38:2435.
[26] Vehoff H, Neumann P. Acta Metall 1980;28:265.
[27] [27] Vehoff H, Rothe W. Acta Metall 1983;31:1781.
[28] Barnoush A, Vehoff H. Acta Mater 2010;58:5274.
[29] Jokl ML, Vitek Jr V, McMahon CJ. Acta Metall 1980;28:1479.
[30] Bruemmer SM, Jones RH, Thomas MT, Baer DR. Metall Trans A 1983:223.
[31] Jones RH, Bruemmer SM, Thomas MT, Baer DR. Metall Trans A 1983;59:1729.
[32] Kameda J, McMahon Jr CJ. Metall Trans A 1983;59:903.
[33] Lassila DH, Birnbaum HK. Acta Metall 1987;35:1815.
[34] Lassila DH, Birnbaum HK. Acta Metall 1988;36:2821.
[35] McMahon Jr CJ. Eng Fract Mech 2001;68:773.
[36] Moody NR, Perra MW, Robinson SL. Scr Metall 1988;22:1261.
[37] Moody NR, Perra MW, Robinson SL. Hydrogen-induced cracking in an iron-based superalloy. In: Moody NR, Thompson AW, editors. Proceedings of the 4th international conference on effect of hydrogen on behavior of materials. Warrendale, PA: TMS; 1990. p. 625.
[38] Teter DF, Robertson IM, Birnbaum HK. Acta Mater 2001;49: 4313.
[39] Dadfarnia M, Novak P, Ahn DC, Liu JB, Sofronis P, Johnson DD, et al. Adv Mater 2010;22:1128.
[40] Jiang DE, Carter EA. Acta Mater 2004;52:4801.
[41] Van der Ven A, Ceder G. Acta Mater 2004;52:1223.
[42] Leiping Z, Ruqian W, Freeman AJ, Olson GB. Phys Rev B 2000;62: 13938.
[43] Hirth JP, Rice JR. Metall Trans A – Phys Metall Mater Sci 1980;11: 1501.
[44] Mishin Y, Sofronis P, Bassani JL. Acta Mater 2002;50:3609.
[45] Lynch SP. Scr Metall 1979;13:1051.
[46] Marchi CS, Somerday BP, Nibur KA, Stalheim DG, Boggess T, Jansto S. Fracture and fatigue of commercial grade API pipeline steels in gaseous hydrogen. In: Pressure vessels & piping division/K-PVP conference. Bellevue, WA: ASME; 2010.
[47] Stalheim DG, Marchi CS, Somerday BP, Sofronis P, Boggess T, Jansto S, Muralidharan G. Microstructure and mechanical property performance of commercial grade API pipeline steels in high pressure gaseous hydrogen. In: 8th International pipeline conference. Calgary; 2010.
[48] Martin ML, Fenske JA, Liu GS, Sofronis P, Robertson IM. Acta Mater 2011;59:1601.
[49] Fenske JA, Robertson IM, Ayer R, Hukle M, Lillig D, Newbury B. Metall Mater Trans, in preparation
[50] Martin M, Robertson IM. Private communication; 2010.
[51] Chen SH, Katz Y, Gerberich WW. Philos Mag A, Phys Condens Matter Defects Mech Prop 1991;63:131.